ЖЭТФ, 2024, том 166, вып. 2 (8), стр. 216–231

EFFECT OF COLOR RANDOMIZATION ON p_T BROADENING OF FAST PARTONS IN TURBULENT QUARK-GLUON PLASMA

B. G. Zakharov*

L. D. Landau Institute for Theoretical Physics of the Russian Academy of Sciences
117334, Moscow, Russia

Received March 12, 2024,
revised version March 12, 2024,
Accepted for publication April 6, 2024

We analyze the effect of the parton color randomization on p_T broadening in the quark-gluon plasma with turbulent color fields. We calculate the transport coefficient for a simplified model of fluctuating color fields in the form of alternating sequential transverse layers with homogenous transverse chromomagnetic fields with random orientation in the SU(3) group and gaussian distribution in the magnitude. Our numerical results show that the color randomization can lead to a sizable reduction of the turbulent contribution to $\hat{q}$. The magnitude of the effect grows with increasing ratio of the electric and magnetic screening masses.

DOI: 10.31857/S0044451024080078

1. INTRODUCTION

The experiments on heavy ion collisions at RHIC and the LHC led to the discovery of quark-gluon plasma (QGP). The hydrodynamic simulations (for reviews, see, e.g., Refs. [1–3]) of AA collisions at the RHIC and LHC energies show that the QGP produced in AA collisions flows as almost ideal fluid with a very small shear viscosity to entropy density ratio η/s, of the order of the lower bound $\eta/s \sim 1/4\pi$ [4]. Hydrodynamical analyses give strong evidence for the onset of the collective flow/thermalization regime of the QCD matter at the proper time $\tau_0 \sim 0.5 - 1$ fm [3, 5]. No clear consensus has emerged on whether these facts can be explained within the paradigm of the weakly coupled QGP. On the one hand, calculations of the shear viscosity in the kinetic theory with $2 \to 2$ parton processes in the leading logarithmic approximation [6] give $\eta/s \sim 0.6$ (for the QCD coupling constant $g = 2$ and $N_F = 2.5$), that is considerably larger than required for description of the flow effects observed in AA collisions at RHIC and the LHC. This contradiction of the kinetic theory with binary collisions to data on AA collisions was confirmed by direct simulation of the QGP evolution in AA collisions at RHIC energies within the Boltzmann equation performed in [7]. The inclusion of the near collinear splitting $1 \leftrightarrow 2$ processes [8] does not change considerably the ratio η/s. However, in [9] it was shown that accounting for the NLO corrections to the formulas of the effective kinetic approach of [8] can considerably reduce η/s [1)]. On the other hand, there is indication that with the inclusion of the large angle $2 \leftrightarrow 3$ processes the kinetic approach may give $\eta/s \sim 1/4\pi$ [11] without the NLO corrections to the parton cross sections. Also, the approach of [11] leads to considerable decrease of the thermalization time [12] as compared to the perturbative "bottom-up" scenario [13] based on the Boltzmann equation with $2 \to 2$ and near collinear $2 \leftrightarrow 3$ processes, which does not explain the small thermalization time. However, one should bear in mind that the analyses [7–9,11–13] ignore the possible plasma instabilities that can appear for anisotropic initial parton system produced in AA collisions [14–16]. Possible importance of the QGP instabilities for AA collisions was first discussed in [17]. One of the important QGP instabilities is the chromomagnetic instability similar to the Weibel instability in the ordinary plasmas [18]. The unstable chromomagnetic modes of the gluon field due to the color Weibel instability must appear due to strong anisotropy of the initial parton distribution [13–15, 19] for which the transverse parton momenta

* E-mail: bgz@itp.ac.ru

[1)] The large difference between LO and NLO results of [9] arises from the large NLO correction to $\hat{q}$ obtained in [10], which is used in the framework of [9] for description of the small angle parton scattering within the Fokker-Plank approximation.

are larger than that along the beam axis. The generation of the unstable color fields can accelerate the thermalization [19, 20]. From the point of view of the flow effects in AA collisions, it is important that interaction of the thermal partons with the random color fields can reduce the parton mean free path in the QGP, and consequently can decrease the viscosity of the QGP produced in AA collisions. This mechanism of generation of a small effective shear viscosity of the QGP in AA collisions has been addressed in Refs. [21–23]. Also, in [24] it was argued that the turbulent color fields in the QGP can potentially be important for spin transport in AA collisions. The effect of the instabilities on the QGP evolution in AA collisions has attracted much attention in the literature (for a review, see Refs. [25, 26]).

The reduction of the QGP shear viscosity in the presence in the QGP of the turbulent collective color fields is closely related to the turbulent enhancement of the transport coefficient $\hat{q}$ [23]. The transport coefficient $\hat{q}$ characterizes the mean squared transverse momentum acquired by a fast particle per unit length in the QGP [27]. In terms of $\hat{q}$ one can obtain the estimate for the typical length, λ, of degradation of the momentum for thermal partons in the QGP: $\lambda = b\langle p\rangle^2/\hat{q}$, where $\langle p\rangle \sim 3T$ is the average parton momentum, and a reasonable choice for the coefficient b is $b \sim 0.5$. Then, using the fact that in the kinetic theory the shear viscosity is approximately [28, 29]

$$\eta \sim \frac{1}{3} n\langle p\rangle\lambda \tag{1}$$

(n is the parton number density) one can obtain the approximate relation between η and $\hat{q}$

$$\frac{\eta}{s} \sim \frac{1.5T^3}{\hat{q}}\,, \tag{2}$$

that agrees reasonably with the estimates given in [23, 30].

Besides the effect of the turbulent contribution to $\hat{q}$ on the QGP shear viscosity, it is also important for p_T broadening of fast partons with energy $E \gg T$ produced in hard processes in AA collisions. Interaction of fast partons with the collective color fields can also lead to synchrotron-like gluon radiation [31], which may enhance jet quenching in AA collisions. The effect of the collective background color fields on the p_T broadening of fast partons in an unstable QGP has been addressed in [32] within the classical approach using Wong's equations [33]. A quantum calculation of p_T broadening of a fast parton in random color fields have been performed in [34] (in the context of the parton p_T broadening in the glasma color fields). The turbulent contribution to $\hat{q}$ is $\propto g^2\epsilon_f r_c$, where ϵ_f is the mean energy density of the turbulent collective fields, and r_c is the correlation length of these fields. This result is natural and quite transparent since p_T broadening arises due to random transverse momentum kicks with $\Delta p_T^2 \sim g^2\epsilon_f r_c^2$. However, the calculations of [32, 34] ignore the fact that gluon exchanges between the fast parton and the QGP constituents can change the color state of the fast parton. It is clear that such gluon exchanges will affect the transverse momentum acquired by the fast parton due to interaction with the collective color field, since the change of the fast parton color state changes the Lorentz force. One can expect that this should reduce the turbulent contribution to p_T broadening, because the color randomization of the fast parton due to the gluon exchanges effectively reduces the correlation length of the Lorentz force in the collective color fields of the QGP. Study of this effect is of interest both from the point of view jet quenching and from the point of view of the turbulent shear viscosity of the QGP [21–23]. The purpose of the present paper is to study this effect quantitatively. We perform calculations for a simplified model of random background chromomagnetic fields with alternate homogeneous field layers.

The paper is organized as follows. In section 2, we give introductory overview of calculations of the contributions to p_T broadening from scattering in turbulent color fields and from scattering on the thermal partons treating these two mechanisms separately. We give a new alternative simple derivation for p_T broadening in the turbulent non-abelian fields. In section 3, we develop a formalism for calculation of p_T broadening in the QGP with fluctuating background fields accounting for the effect of the color randomization of fast partons. In section 4, we present the results of numerical simulations. Conclusions are contained in section 5.

2. TURBULENT AND THERMAL CONTRIBUTIONS TO p_T BROADENING

In this section we discuss briefly the quantum formalism for transverse momentum broadening of fast particles passing through high-temperature QED and QCD plasmas. The approach is similar to that used in our previous studies on the propagation of positronium atoms through a matter [35] and on the Landau-Pomeranchuk-Migdal effect in QED and QCD [36].

We assume that the plasma is statistically homogeneous and isotropic. We consider a fast particle with $E \gg m$ with the initial momentum along the z-axis. At

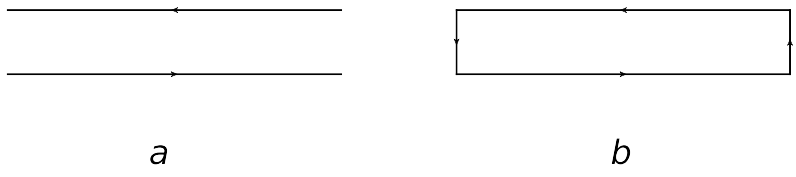

Fig. 1. (a) The lightlike Wilson lines corresponding to the evolution operator for the transverse density matrix of a fast particle in the eikonal approximation; (b) the closed Wilson loop made of the two lightlike Wilson lines and the transverse segments arising from the Aharonov-Bohm phase factors in the initial and final density matrices

leading order in the particle energy E, the transverse dynamics of fast particles in an external field can be described in terms of a 2D Schrödinger equation, which governs the z-evolution (on the light-cone $t-z$ =const) of the transverse wave function [35, 36]. In the transverse Hamiltonian the role of "mass" is played by the particle energy E. The transverse Green function can be written in the Feynman path integral form [37]

$$K(\boldsymbol{\rho}_2, z_2|\boldsymbol{\rho}_1, z_1) = \int D\boldsymbol{\rho}\times \\ \times \exp\left[i\int\limits_{z_1}^{z_2} dz \frac{M(d\boldsymbol{\rho}/dz)^2}{2}\right] W(\{\boldsymbol{\rho}\}), \quad (3)$$

where $M = E$, and

$$W(\{\boldsymbol{\rho}\}, z_2, z_1) = \\ = \exp\left[-ie\int\limits_{z_1}^{z_2} dz\left(A^0 - A^3 - \mathbf{A}_\perp\cdot\mathbf{v}_\perp\right)\right] \quad (4)$$

is the Wilson line factor for the trajectory $\boldsymbol{\rho}(z)$ in the external potential $A_\mu(t, \boldsymbol{\rho}(z), z)$ at $t - z$ =const. In the high energy limit the transverse motion is frozen and the Green function takes the eikonal form (for an abelian external field)

$$K(\boldsymbol{\rho}_2, z_2|\boldsymbol{\rho}_1, z_1) = \delta(\boldsymbol{\rho}_2 - \boldsymbol{\rho}_1) W(\boldsymbol{\rho}, z_2, z_1), \quad (5)$$

where

$$W(\boldsymbol{\rho}, z_2, z_1) = \exp\left[-ie\int\limits_{z_1}^{z_2} dz n^\mu A_\mu\right] = \\ = \exp\left[-ie\int\limits_{z_1}^{z_2} dz(A^0 - A^3)\right] \quad (6)$$

is the lightlike Wilson line factor with $n^\mu = (1, 0, 0, 1)$ for $\boldsymbol{\rho} = \boldsymbol{\rho}_1 = \boldsymbol{\rho}_2$.

In the present analysis we will discuss p_T broadening in the eikonal approximation. However, using the path integral representation (3) for the Green functions, one can show that for statistically transverse uniform medium the calculations of p_T broadening with accurate Green functions give the same results as the eikonal approximation [35, 36]. For this reason, all the results presented in this paper remain valid beyond the eikonal approximation.

2.1. p_T broadening in turbulent background fields

2.1.1. Abelian field

Let us consider first a charged particle propagating in a fluctuating electromagnetic field. For a given external field, the evolution operator for the transverse density matrix $\rho(\mathbf{b}, \mathbf{b}', z) = \phi(\mathbf{b}, z)\phi^*(\mathbf{b}', z)$ (hereafter we denote the transverse vectors with bold letters) in the eikonal approximation (corresponding to the diagram of Fig. 1a) reads

$$S(\mathbf{b}, \mathbf{b}', z_2|\mathbf{b}, \mathbf{b}', z_1) = W(\mathbf{b}, z_2, z_1) W^*(\mathbf{b}', z_2, z_1) = \\ = W(\mathbf{b}, z_2, z_1) W(\mathbf{b}', z_1, z_2), \quad (7)$$

where $W(\mathbf{b}, z_2, z_1)$ and $W(\mathbf{b}', z_1, z_2)$ are the lightlike Wilson line factors given by (6) corresponding to the paths from $(\mathbf{b}, z_1)$ to $(\mathbf{b}, z_2)$ and $(\mathbf{b}', z_2)$ to $(\mathbf{b}', z_1)$, respectively. The first equality in (7) shows that, formally, the operator S can also be viewed as the eikonal S-matrix for scattering of e^+e^- pair. Below this fact will be used to express the thermal contribution to $\hat{q}$ in terms of the dipole cross section $\sigma_{e^+e^-}$ (or $\sigma_{q\bar{q}}$ for the QGP) as was done in [35, 36]. But for p_T broadening in turbulent fields we treat S as the evolution operator of the density matrix.

For statistically uniform medium, the value of $(\mathbf{b} + \mathbf{b}')/2$ is immaterial, and one can take $\mathbf{b} = -\boldsymbol{\rho}/2$ and $\mathbf{b}' = \boldsymbol{\rho}/2$ for the eikonal lightlike lines. We take $z_1 = 0$ and $z_2 = L$. We will consider the evolution operator as a function of $\boldsymbol{\rho}$ and L. The transverse momentum distribution, $I(\mathbf{p})$, of the final particle (for the

initial state with zero transverse momentum) can be written in terms of the operator S as

$$I(\mathbf{p}) = \frac{1}{(2\pi)^2}\Big\langle\Big\langle\langle\rho_{\mathbf{p}}|S|\rho_0\rangle\Big\rangle\Big\rangle, \tag{8}$$

where $\Big\langle\Big\langle\ldots\Big\rangle\Big\rangle$ means averaging over the ensemble of the background fields, ρ_0 is the density matrix of the initial state with zero transverse momentum, and $\rho_{\mathbf{p}}$ is the density matrix of the final particle with transverse momentum $\mathbf{p}$. We assume that at $z = z_{1,2}$ the magnetic field vanishes, i.e., $\mathbf{A}_\perp$ is pure gauge. The density matrix of a particle with the physical transverse momentum $\mathbf{p}$ in the presence of a non-zero pure gauge transverse vector potential $\mathbf{A}_\perp$ reads

$$\rho_{\mathbf{p}}(z_2,\boldsymbol{\rho}) = \exp\left[-i\mathbf{p}\boldsymbol{\rho}\right]\cdot W^*(\boldsymbol{\rho}/2,-\boldsymbol{\rho}/2,z_2), \tag{9}$$

where

$$W(\mathbf{b}',\mathbf{b},z) = \exp\left[ie\int\limits_{\mathbf{b}}^{\mathbf{b}'} d\boldsymbol{\tau}\mathbf{A}_\perp\right] \tag{10}$$

is the Wilson line factor for the straight transverse path from $\mathbf{b}$ to $\mathbf{b}'$, which appears due to the Aharonov-Bohm phase shift [38]. Note that in the presence of a real magnetic field, when $\mathbf{A}_\perp$ is not pure gauge, the final particle can not be regarded as having a definite transverse momentum. In this case, $\mathbf{p}$ can only be determined with uncertainty of the order of the inverse Larmor radius (which corresponds to the relative error $\Delta p/p \sim eB/p^2$).

Using (7), (8) and (9) one can write the momentum distribution of the final parton as

$$I(\mathbf{p}) = \frac{1}{(2\pi)^2}\int d\boldsymbol{\rho}\exp[i\mathbf{p}\boldsymbol{\rho}]\Big\langle\Big\langle W_c(\boldsymbol{\rho},L)\Big\rangle\Big\rangle, \tag{11}$$

where W_c is the Wilson factor for the closed path as shown in Fig. 1b, which includes the two straight lightlike lines and the two transverse segments (corresponding to the Aharonov-Bohm phase factors in the initial and final density matrices)

$$\begin{aligned} W_c(\boldsymbol{\rho},L) &= W(-\boldsymbol{\rho}/2,z_1,z_2)W(\boldsymbol{\rho}/2,-\boldsymbol{\rho}/2,z_2)\times \\ &\times W(\boldsymbol{\rho}/2,z_2,z_1)W(-\boldsymbol{\rho}/2,\boldsymbol{\rho}/2,z_1) \\ &= \exp\left[-ie\oint\limits_C dx^\mu \hat{A}_\mu\right] \end{aligned} \tag{12}$$

with $z_1 = 0$, $z_2 = L$. The definition of p_T broadening in the QGP in terms of the closed lightlike Wilson loop was suggested in [39, 40] in strong-coupling calculations of $\hat{q}$ using AdS/CFT correspondence. In [39,40], it was assumed that p_T broadening is associated with the long lightlike Wilson lines, and the effect of two short transverse segments can be ignored. However, one should be in mind that in some cases the whole effect of p_T broadening may come from the transverse Wilson lines. For instance, this occurs for a fluctuating transverse magnetic field described by a z-dependent transverse vector potential: $\mathbf{B} = \nabla\times\mathbf{A}_\perp(z)$. In this case the lightlike Wilson factors equal unity, and p_T broadening arises due to fluctuating Aharonov-Bohm phases in the transverse Wilson factors (or in one of them). This occurs even if the transverse Wilson lines are located outside the medium.

We write the averaged W_c in the form

$$\Big\langle\Big\langle W_c(\boldsymbol{\rho},L)\Big\rangle\Big\rangle = \exp[-P(\boldsymbol{\rho})]. \tag{13}$$

In terms of the function $P(\boldsymbol{\rho})$, $I(\mathbf{p})$ reads

$$I(\mathbf{p}) = \frac{1}{(2\pi)^2}\int d\boldsymbol{\rho}\exp\left[i\mathbf{p}\boldsymbol{\rho} - P(\boldsymbol{\rho})\right]. \tag{14}$$

The value of $\langle\mathbf{p}^2\rangle$ is sensitive to the behavior of $P(\boldsymbol{\rho})$ at small ρ. For particle scattering in the collective turbulent fields we have $P(\boldsymbol{\rho}) \propto \rho^2$ in the limit $\rho\to 0$. In this case, from (14) one obtains

$$\langle\mathbf{p}^2\rangle = \boldsymbol{\nabla}^2 P(\boldsymbol{\rho})\Big|_{\rho=0} = \lim_{\rho\to 0} 4P(\rho)/\rho^2. \tag{15}$$

The integral over the closed contour $\oint_C dx^\mu A_\mu$ in (12) can be transformed in an integral over the surface spanning it with the help of the Stokes theorem

$$\oint_C dx^\mu A_\mu = \frac{1}{2}\int d\sigma^{\mu\nu}F_{\mu\nu}. \tag{16}$$

In the limit of small $\boldsymbol{\rho}$, the surface integral on the right hand side of (16) can be written as

$$\frac{1}{2}\int d\sigma^{\mu\nu}F_{\mu\nu} \approx \int\limits_0^L dz\boldsymbol{\rho}^j F_{j+}, \tag{17}$$

where $j = 1, 2$ is the transverse index. Using (17) one obtains at small $\boldsymbol{\rho}$

$$P(\boldsymbol{\rho}) \approx \frac{\boldsymbol{\rho}^2 e^2}{4}\int\limits_0^L dz\int\limits_0^L dz'\Big\langle\Big\langle F_{i+}(z)F_{i+}(z')\Big\rangle\Big\rangle, \tag{18}$$

where, for brevity, for F_{i+} we indicate only the longitudinal component z of the position four-vector $x^\mu = (z,0,0,z)$. Assuming that the field correlation radius, r_c, is small compared to the medium thickness L, from (15) and (18) one obtains

$$\langle\mathbf{p}^2\rangle = 2Le^2\int\limits_0^\infty dz\Big\langle\Big\langle F_{i+}(z)F_{i+}(0)\Big\rangle\Big\rangle. \tag{19}$$

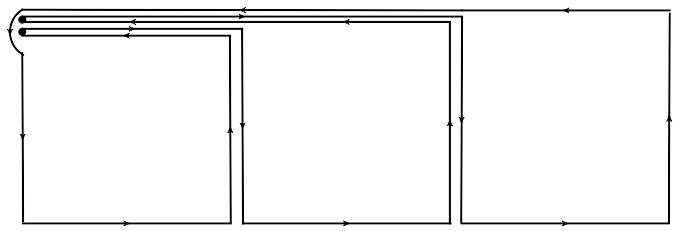

Fig. 2. A cartoon depicting the deformation of the rectangular Wilson loop of Fig. 1b to rewrite the closed non-abelian Wilson line operator in terms of a surface integral

This formula can be rewritten as

$$\langle \mathbf{p}^2 \rangle = 2L \int\limits_0^\infty dz \Big\langle \Big\langle f_i(z) f_i(0) \Big\rangle \Big\rangle , \tag{20}$$

where $f_i(z) = -eF_{i+}(z)$ is the ith component of the Lorentz force experienced by the charged particle with velocity $v \approx 1$ along z axis. The formulas (19) and (20) are consistent with the physical picture of p_T broadening as a random walk in the tranverse momentum arising from the transverse momentum kicks with $\langle \Delta \mathbf{p}^2 \rangle \sim e^2 \epsilon_f r_c^2$ in scatterings on the domains of the background fields.

2.1.2. Non-abelian field

Consider now p_T broadening in the non-abelian turbulent collective color fields. It was addressed previously in [32, 34]. Here we give an alternative simple derivation very similar to that given above for the abelian case. In the non-abelian case, the external potential in the Wilson lines shown in Fig. 1 becomes the color operator $A_\mu = A_\mu^a \mathbf{T}_R^a$, where $\mathbf{T}_R^a$ is the color SU(3) generator for the fast parton. And the abelian formula (12) is now replaced by

$$\mathrm{Tr} W_c = \mathrm{Tr} \left[\mathcal{P} \exp \left(-ig \oint\limits_C dx^\mu A_\mu^a \mathbf{T}_R^a \right) \right] , \tag{21}$$

where $\mathcal{P}$ denotes path ordering of the exponential. We assume that the beginning and the end of the path C are at the upper left corner of the rectangular contour shown in Fig. 1b. The non-abelian function $P(\boldsymbol{\rho})$ is defined as

$$\frac{1}{d_R} \Big\langle \Big\langle \mathrm{Tr} W_c(\boldsymbol{\rho}, L) \Big\rangle \Big\rangle = \exp[-P(\boldsymbol{\rho})] , \tag{22}$$

where d_R is the dimension of the color representation for the fast parton i.e., for SU(3) $d_R = 3$ and 8 for quarks and gluons, respectively.

The Wilson line operator W_c can be rewritten in terms of a surface integral with the help of the non-abelian Stokes theorem [41–44]. For small $\boldsymbol{\rho}$ this can be done using the deformation of the contour C to the one with a sequence of small plaquettes as shown in Fig. 2. Then, we obtain

$$[W_c]_j^i = \mathcal{P}_n \Big[\prod_{n=1}^N U(z_n) \Big]_j^i , \tag{23}$$

$$[U(z_n)]_j^i \approx \delta_j^i - \\ - \frac{ig}{2} \Delta \sigma^{\mu\nu} F_{\mu\nu}^a(z_n) [\Omega_R^+(z_n) \mathbf{T}_R^a \Omega_R(z_n)]_j^i , \tag{24}$$

$$\Omega_R(z_n) = \mathcal{P} \exp \left[-ig \int\limits_0^{z_n} dz n^\mu A_\mu^a(z) \mathbf{T}_R^a \right] . \tag{25}$$

In (23)–(25) and below we suppress the time component ($x^0 = z$) and the transverse components ($\mathbf{x}_\perp^{1,2} = 0$) of the position four-vectors in arguments of $F_{\mu\nu}^a$ and A_μ^a for notational simplicity. One can rewrite (24) as

$$U(z_n) = \hat{1} - \frac{ig}{2} \Delta \sigma^{\mu\nu} \tilde{F}_{\mu\nu}^a(z_n) \mathbf{T}_R^a , \tag{26}$$

where $\tilde{F}_{\mu\nu} = \Omega_A^+ F_{\mu\nu}$ is the color rotated field strength tensor. Using (23), (26) and (21) one obtains

$$\mathrm{Tr} W_c \Big|_{\boldsymbol{\rho} \to 0} \approx \\ \approx \mathrm{Tr} \left[\mathcal{P} \exp \left(-ig \boldsymbol{\rho}^j \int\limits_0^L dz \tilde{F}_{j+}^a(z) \mathbf{T}_R^a \right) \right] . \tag{27}$$

Then, using the relation $\mathrm{Tr}(\mathbf{T}_R^a \mathbf{T}_R^b) = \delta^{ab} d_R C_R / (N_c^2 - 1)$, from (27) and (15) we obtain the non-abelian counterparts of (18) and (19)

$$P(\boldsymbol{\rho}) \approx \frac{\boldsymbol{\rho}^2 g^2 C_R}{2(N_c^2 - 1)} \times \\ \times \int\limits_0^L dz_1 \int\limits_0^{z_1} dz_2 \Big\langle \Big\langle \tilde{F}_{i+}^a(z_1) \tilde{F}_{i+}^a(z_2) \Big\rangle \Big\rangle , \tag{28}$$

$$\langle \mathbf{p}^2 \rangle = \frac{2Lg^2 C_R}{N_c^2 - 1} \int\limits_0^\infty dz \Big\langle \Big\langle \tilde{F}_{i+}^a(z) \tilde{F}_{i+}^a(0) \Big\rangle \Big\rangle . \tag{29}$$

2.2. Thermal contribution to p_T broadening

2.2.1. Abelian plasma

Consider now the thermal contribution to p_T broadening for charged particles in the QED plasma due to multiple scattering on the plasma constituents. The thermal contribution to p_T broadening in the QED plasma can be treated similarly to the case of ordinary amorphous materials addressed in [35]. The function P corresponding to the product WW^* of the Wilson factors for the diagram of Fig. 1a, can be expressed through the Wightman photon field correlator $\langle\langle A^\mu(x)A^\nu(y)\rangle\rangle$ as

$$P_{th}(\boldsymbol{\rho}) = e^2 L \int\limits_{-\infty}^{\infty} dz[G(z,0_\perp z) - G(z,\boldsymbol{\rho},z)]\,, \qquad (30)$$

$$G(x-y) = n^\mu n^\nu \langle\langle A_\mu(x)A_\nu(y)\rangle\rangle\,. \qquad (31)$$

In the approximation of the static Debye screened Coulomb centers (similar to that of [45] for the QGP), neglecting correlations between the plasma constituents, the function $P_{th}(\boldsymbol{\rho})$ given by (30) can be written as

$$P^{st}_{th}(\boldsymbol{\rho}) = \frac{Ln\sigma_{e^+e^-}(\rho)}{2}\,, \qquad (32)$$

where $n = 3\xi(3)T^3/\pi^2$ is the number plasma density (for the electron-positron plasma with zero chemical potential, and $T \gg m_e$), and $\sigma_{e^+e^-}(\rho)$ is the dipole cross section for scattering of the e^+e^- pair on the scattering center. In the two-photon exchange approximation $\sigma_{e^+e^-}(\rho)$ reads

$$\sigma_{e^+e^-}(\rho) = \frac{e^4}{2\pi^2}\int d\mathbf{q}\frac{[1-\exp(i\mathbf{q}\boldsymbol{\rho})]}{(\mathbf{q}^2+m_D^2)^2}\,, \qquad (33)$$

where $m_D = eT/\sqrt{3}$ is the Debye mass for the QED plasma [46]. The formula (33) corresponds to the function $P_{th}(\boldsymbol{\rho})$

$$P^{st}_{th}(\boldsymbol{\rho}) = \frac{1}{(2\pi)^2}\int d\mathbf{q}[1-\exp(i\mathbf{q}\boldsymbol{\rho})]P^{st}_{th}(\mathbf{q}) \qquad (34)$$

with

$$P^{st}_{th}(\mathbf{q}) = \frac{Le^4 3\xi(3)T^3}{\pi^2(q^2+m_D^2)^2}\,. \qquad (35)$$

The ratio

$$C_2(\rho) = \sigma_{e^+e^-}/\rho^2$$

(and $P^{st}_{th}(\rho)/\rho^2$) has a logarithmic dependence $\propto \ln(1/\rho m_D)$ at $\rho \ll 1/m_D$ due to the Coulomb tail in scattering on the plasma constituents at $q^2 \gtrsim m_D^2$. Due to the appearance of the Coulomb logarithm, for the thermal contribution the prescription (15) is replaced by

$$\langle \mathbf{p}^2\rangle \approx \boldsymbol{\nabla}^2 P(\boldsymbol{\rho})\Big|_{\rho\sim\rho_{min}} \approx 4P(\rho_{min})/\rho^2_{min}\,, \qquad (36)$$

where $\rho_{min} \sim 1/q_{max}$, and q_{max} is the maximal momentum transfer for $2\to 2$ scattering of the fast particle on the plasma constituents (for a relativistic plasma $q^2_{max} \sim 6ET$). The transport coefficient

$$\hat{q} = d\langle \mathbf{p}^2\rangle/dL$$

in terms of the function C_2 reads

$$\hat{q}^{st}_{th} = 2nC_2(\rho\sim\rho_{min})\,. \qquad (37)$$

The Coulomb tail leads to a logarithmic increase of $\hat{q}_{th}$ with the particle energy. In the static model, from (34), (35) and (36) for $\hat{q}_{th}$ in the leading-logarithmic (LL) approximation one obtains

$$\hat{q}^{st}_{th} \approx \frac{e^4 3\xi(3)T^3}{4\pi^3}\ln\left(\frac{6ET}{m_D^2}\right)\,. \qquad (38)$$

In the HTL scheme [47] the $P_{th}(\mathbf{q})$ can be written as

$$P^{HTL}_{th}(\mathbf{q}) = Le^2TC(\mathbf{q}) \qquad (39)$$

with

$$C(\mathbf{q}) = \frac{m_D^2}{q^2(q^2+m_D^2)},$$

see Ref. [48]. This gives the HTL transport coefficient in the LL approximation

$$\hat{q}^{HTL}_{th} \approx \frac{e^4T^3}{12\pi}\ln\left(\frac{6ET}{m_D^2}\right)\,. \qquad (40)$$

In the HTL scheme the coefficient of the logarithm in $\hat{q}_{th}$ is smaller by a factor of $\pi^2/9\xi(3) \approx 0.912$. This difference is not surprising since the HTL scheme is assumed to be valid only at the momenta $\sim eT \ll T$. In principle, since the Coulomb logarithm comes from the broad region $6ET \gtrsim q^2 \gtrsim m_D^2$, the prediction of the static model for $\hat{q}_{th}$ should be more accurate than that of the HTL scheme at $E \gg m_D^2/T$. Because in this regime the coefficient of the logarithm is controlled by the number density of the plasma, and this is clearly fulfilled in the static model.

Note that for the QED plasma the turbulent and thermal contributions to $\hat{q}$ are additive, since these two mechanisms do not affect each other.

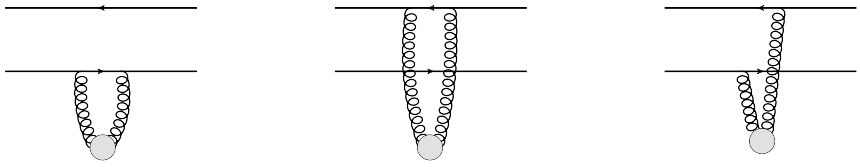

Fig. 3. Diagrams describing the dipole operator (41) for scattering of $p\bar{p}$ pair on the plasma constituent in the double-gluon approximation

2.2.2. Non-abelian plasma

Calculation of the thermal p_T broadening in the QGP is very similar that for the QED plasma. Similarly to QED, we can view the upper line $\leftarrow$ in Fig. 1a as the Wilson line for antiparticle $\bar{p}$, since in QCD for a particle p (quark or gluon) in the color representation R, $-(T^a_R)^*$ equals the color generator $T^a_{\bar{R}}$ for $\bar{p}$. Then, similarly to QED, the evolution operator of the non-abelian density matrix can be viewed as S-matrix for a fictitious $p\bar{p}$ state. This is valid if we restrict ourselves to contributions of one- and two-gluon exchanges between fast partons and plasma constituents (as shown in Fig. 3).

In the approximation of the static Debye screened color centers [45], the two-gluon exchange amplitude of Fig. 3 acts as a color operator

$$\langle p^\beta, \bar{p}^{\bar{\beta}}|\hat{\sigma}(\boldsymbol{\rho})|p^\alpha, \bar{p}^{\bar{\alpha}}\rangle = \\ = \frac{C_R C_t g^4}{16\pi^2}\int d\mathbf{q}\frac{1}{(q^2+m_D^2)^2}\times \\ \times\Big[\delta^\beta_\alpha\delta^{\bar{\beta}}_{\bar{\alpha}} - (T^a_R)^\beta_\alpha (T^a_{\bar{R}})^{\bar{\beta}}_{\bar{\alpha}}\frac{\exp(i\mathbf{q}\cdot\boldsymbol{\rho})}{C_R}\Big], \quad (41)$$

where $m_D = gT\sqrt{1+N_F/6}$ is the Debye mass, and C_R and C_t are the Casimir color operators of the fast parton and of the QGP constituent. This formula accounts for that in Fig. 3, due to sum over the color indices of the plasma constituent, the two-gluon t-channel states are color singlets. This fact guarantees that, after summing over the color indices for the initial/final $p\bar{p}$ states, all the intermediate $p\bar{p}$ states between scatterings on different QGP constituents are color singlets. This allows one in calculating the function P to replace the dipole operator (41) by its expectation value between the color singlet $p\bar{p}$ states, i.e., by the dipole cross-section

$$\sigma^t_{p\bar{p}}(\boldsymbol{\rho}) = \langle\{1\}|\hat{\sigma}(\boldsymbol{\rho})|\{1\}\rangle = \\ = \frac{C_R C_t g^4}{16\pi^2}\int d\mathbf{q}\frac{1}{(q^2+m_D^2)^2}\Big[1-\exp(i\mathbf{q}\cdot\boldsymbol{\rho})\Big]. \quad (42)$$

Then, one obtains for the QCD counterpart of (32)

$$P^{st}_{th}(\boldsymbol{\rho}) = \frac{L\sum_{t=q,g} n_t\sigma^t_{p\bar{p}}(\rho)}{2} = \frac{Ln^{eff}_q\sigma^q_{p\bar{p}}(\rho)}{2}, \quad (43)$$

where $n_{q,g}$ are the thermal number densities of quarks and gluons, and n^{eff}_q is defined as

$$n^{eff}_q = n_q + n_g C_A/C_F = \\ = \xi(3)[N_F 9 + C_A 16/C_F]T^3/\pi^2. \quad (44)$$

Calculating

$$C_2(\rho_{min}) = \sigma^q_{p\bar{p}}(\rho_{min})/\rho^2_{min}$$

in the LL approximation one obtains the thermal transport coefficient for the static model

$$\hat{q}^{st}_{th} \approx \frac{g^4 C_R\xi(3)[C_F N_F 9 + C_A 16]T^3}{32\pi^3}\ln\Big(\frac{6ET}{m_D^2}\Big). \quad (45)$$

In the HTL scheme we have

$$P^{HTL}_{th}(\mathbf{q}) = Lg^2 C_R T C(\mathbf{q}), \quad (46)$$

and the transport coefficient in the LL approximation is given by

$$\hat{q}^{HTL}_{th} \approx \frac{g^4 C_R T^3[1+N_F/6]}{4\pi}\ln\Big(\frac{6ET}{m_D^2}\Big). \quad (47)$$

Comparing (47) and (45) one sees that in the LL approximation the ratio of $\hat{q}_{th}$ for the HTL scheme to that for the static model is

$$\frac{\pi^2(1+N_f/6)}{6\xi(3)(1+N_f/4)} \approx 1.19 \text{ for } N_f = 2.5.$$

Contrary to the QED plasma for the QGP the contributions to p_T broadening of the thermal and of the background field mechanisms are non-additive, since p_T broadening due to the background field is modified because the color exchanges between the fast parton and the medium constituents lead to change of the Lorentz force experienced by the fast parton in the background color field. For this reason, the two mechanisms of p_T broadening in the QGP must be treated on an even footing.

3. p_T BROADENING OF FAST PARTONS IN THE QGP WITH SIMULTANEOUS TREATMENT OF THERMAL AND BACKGROUND FIELD EFFECTS

In this section we study the non-additivity of p_T broadening in the QGP corresponding to the background field and to the thermal mechanisms for a simplified model of the random background field. We consider the case of fluctuating layered background color magnetic field with the transverse layers. We assume that in each layer the magnetic field is purely transverse and homogeneous. The fields in different layers are assumed to be uncorrelated. In this model the layer thickness, ΔL, plays the role of the field correlation radius in the real turbulent QGP. The assumption of a purely transverse (and magnetic) field does not seem to be too restrictive, since for p_T broadening the crucial quantity is the transverse Lorentz force acting on the fast parton. We consider a brick of QGP with $N \gg 1$ slabs (i.e., with $L \gg \Delta L$) of fluctuating homogeneous transverse color magnetic field $\mathbf{B}^a$. The fields in different slabs are assumed to be uncorrelated. For the thermal QGP constituents we use the model of the Debye screened color centers [45] with the dipole color operator given by (41). Also, we present the results treating scattering of the fast parton on the thermal fluctuations for the HTL scheme with a non-zero magnetic screening mass [48]. In each slab we take the external vector potential in the form

$$A^{a\mu} = (0, 0, 0, [\mathbf{B}^a \times \boldsymbol{\rho}]^3) = (0, 0, 0, \boldsymbol{\rho} \cdot \mathbf{f}^a)\,. \qquad (48)$$

where $\mathbf{B}^a$ is the transverse chromomagnetic field, and $\mathbf{f}^a$ is the transverse Lorentz force for $g = 1$. We assume that the vector potential is absent at the initial and final points of the lightlike Wilson lines of Fig. 1a, and consequently the tranverse Wilson factors can be omitted. We treat the complex conjugated lightlike Wilson factor of the parton p as that of $\bar{p}$.

Our starting point is the evolution operator for the transverse density matrix for the set $\{f\} = (f_1, ..., f_N)$ of the Lorentz forces acting in the layers $1, \ldots, N$, written as

$$S(\boldsymbol{\rho}, L, \{f\}) = W_p(-\boldsymbol{\rho}/2, L, \{f\}) W_{\bar{p}}(\boldsymbol{\rho}/2, L, \{f\})\,. \qquad (49)$$

The transverse momentum distribution $I(\mathbf{p})$ can be written as

$$I(\mathbf{p}) = \frac{1}{(2\pi)^2} \times \\ \times \int d\boldsymbol{\rho} \exp[i\mathbf{p} \cdot \boldsymbol{\rho}] \Big\langle\Big\langle \langle\{1\}|S(\boldsymbol{\rho}, L, \{f\})|\{1\}\rangle \Big\rangle\Big\rangle\,, \qquad (50)$$

where $|\{1\}\rangle$ is the color singlet wave function of the $p\bar{p}$ pair, and $\Big\langle\Big\langle \ldots \Big\rangle\Big\rangle$ means averaging over the ensemble of the fluctuating chromomagnetic fields and of the positions of the scattering centers. These two averagings can be performed independently. The averaging over the chromomagnetic fields is equivalent to averaging over the vectors of the color Lorentz forces $\mathbf{f}$ for all the layers. For a given set $\{f\}$ of the Lorentz forces in the slabs, the expectation value of the evolution operator S between the color singlet initial and final $p\bar{p}$ states can be written as

$$\langle\{1\}|S(\boldsymbol{\rho}, L, \{f\})|\{1\}\rangle = \\ = \sum_{\Psi_1, \ldots, \Psi_{N-1}} \langle\{1\}|s(\boldsymbol{\rho}, z_{N+1}, z_N, f_N)|\Psi_{N-1}\rangle ... \times \\ \times \langle\Psi_2|s(\boldsymbol{\rho}, z_2, z_1, f_2)|\Psi_1\rangle\langle\Psi_1|s(\boldsymbol{\rho}, z_1, z_0, f_1)|\{1\}\rangle\,, \qquad (51)$$

where

$$z_i = z_1 + \Delta L(i-1),$$

$\Delta L = L/N$ is the slab thickness, f_i is the Lorentz force in the slab i (we omit the transverse space and color indices), and $s(\boldsymbol{\rho}, z_{i+1}, z_i, f_i)$ is the evolution operator for a slab of the QGP in the interval (z_i, z_{i+1}) with the Lorentz force f_i. For each of the $i = 1, ...N$ slabs, by a proper SU(3) rotation U_i, one can transform the color Lorentz force vector f_i^a to the one with components in the Cartan subalgebra (i.e., with nonzero components only for $a = 3$ and $a = 8$). Of course, the necessary matrices U_i may differ for different layers. Assuming that the background color fields in different slabs are uncorrelated, the averaging over the background fields can be performed by independent integrations over the SU(3) rotations U_i of the Cartan vectors f_i for each of the slabs, and subsequent averaging over the Cartan vectors f_i in each layer. Fortunately, one can avoid integrations over the SU(3) rotations U_i. We use the fact that for any color operator O, depending on the color vector f, the color wave function $|\Psi\rangle$ defined as

$$|\Psi\rangle = \int dU O(Uf)|\{1\}\rangle \qquad (52)$$

can contain only color singlet states. This means that in calculating the averaged over the chromomagnetic fields expectation value of the operator S, on the right hand side of (51) all the intermediate color states Ψ_i can be replaced by the color singlet state $\{1\}$. After this replacement, due to the relations

$$\langle\{1\}|s(\boldsymbol{\rho}, z_{i+1}, z_i, U_i f_i)|\{1\}\rangle = \\ = \langle\{1\}|U_i s(\boldsymbol{\rho}, z_{i+1}, z_i, f_i) U_i^{-1}|\{1\}\rangle = \\ = \langle\{1\}|s(\boldsymbol{\rho}, z_{i+1}, z_i, f_i)|\{1\}\rangle\,, \qquad (53)$$

we can exclude all the SU(3) rotation operators U_i. Thus, we are left only with averaging over the Cartan color vectors f_i^a with $a = 3, 8$. Since the integrations over the Cartan vectors are independent in different layers, we obtain

$$\left\langle\left\langle \langle\{1\}|S(\boldsymbol{\rho}, L, \{f\})|\{1\}\rangle \right\rangle\right\rangle = \\ = \left[\left\langle\left\langle \langle\{1\}|s(\boldsymbol{\rho}, \Delta L, 0, f)|\{1\}\rangle \right\rangle\right\rangle_f\right]^N, \quad (54)$$

where $\left\langle\left\langle \dots \right\rangle\right\rangle_f$ means averaging over the Cartan vectors f. Note that the above formulas remain valid if we include averaging over the positions of the color centers (corresponding to the thermal part of p_T broadening) since for the double-gluon exchange amplitude (shown in Fig. 3) the t-channel gluons are in the color singlet state. Thus, in our model the problem is reduced to calculation of the scattering matrix for a single slab of the QGP with a homogeneous background chromomagnetic field. We perform calculations for the Gaussian distributions of the Cartan components of the Lorentz force color vectors $\mathbf{f}_a$ with $a = 3, 8$

$$\frac{1}{\pi\sigma^2} \exp\left(-\frac{\mathbf{f}_a{}^2}{\sigma^2}\right). \quad (55)$$

The interaction of quarks with the Cartan background fields $f_{3,8}$ is diagonal, i.e., it changes only the phase of the $q\bar{q}$ wave function. But it is not the case for gluons. To diagonalize the interaction of gluons with the background field, as in [31], we use the gluon states having definite color isospin, Q_A, and color hypercharge, Q_B, (we will denote the color charge by the two-dimensional vector $Q = (Q_A, Q_B)$). The diagonal color gluon states, in terms of the usual gluon vector potential, G_a $(a = 1 \dots, 8)$, read (the Lorentz indices are omitted)

$$X = (G_1 + iG_2)/\sqrt{2} \quad (Q = (-1, 0)),$$
$$Y = (G_4 + iG_5)/\sqrt{2} \quad (Q = (-1/2, -\sqrt{3}/2)),$$
$$Z = (G_6 + iG_7)/\sqrt{2} \quad (Q = (1/2, -\sqrt{3}/2).$$

The neutral gluons $A = G_3$ and $B = G_3$ have $Q = (0, 0)$, and do not interact with the background field. Note that, despite the fact that the initial $p\bar{p}$ state is the color singlet (due to the contraction of the color indices) after propagation through the background field the non-singlet components appear, nevertheless the total color charge $Q_p + Q_{\bar{p}}$ of the $p\bar{p}$ pair remains zero.

We assume that the two-gluon operator (41) can be viewed as a local in the longitudinal coordinate z (this is the standard assumption in models of jet quenching). In this approximation one can ignore the overlap in the coordinate z of the background field effects and the two-gluon exchanges on the $p\bar{p}$ state. We divide the z-interval $(0, \Delta L)$ into a linear grid of M cells with width $h = \Delta L/M$. We assume that the two-gluon exchanges can only occur in the middle of the cells, i.e., at the transverse slices

$$z_i = \Delta L(i - 1/2)/M, \ i = 1, \dots M.$$

The background field, that acts outside of these slices, changes only the phase of the intermediate $p\bar{p}$ states. We will denote the color wave functions of the intermediate $p\bar{p}$ states in the chromomagnetic field as ψ. Since the external field does not change the total color charge we have only $p\bar{p}$ states with $Q_p + Q_{\bar{p}} = 0$. The phase factor for the intermediate $p\bar{p}$ pair in a color state ψ after propagating trough the medium a distance Δz reads

$$\Phi_\psi(\Delta z, Q, \boldsymbol{\rho}, f) = \exp\left[ig\Delta z\boldsymbol{\rho}^i \sum_{a=3,8} Q^a f_i^a\right], \quad (56)$$

where

$$Q^a = (Q_p^a - Q_{\bar{p}}^a)/2 = Q_p^a.$$

For quarks we have 3 types of the color neutral $q\bar{q}$ intermediate states:

$$q^1\bar{q}^1 \quad (Q = (1/2, 1/2\sqrt{3})),$$
$$q^2\bar{q}^2 \quad (Q = (-1/2, 1/2\sqrt{3})),$$
$$q^3\bar{q}^3 \quad (Q = (0, -1/\sqrt{3})).$$

For gluons (in the basis of charged and neutral gluons) we have 10 types of the color neutral $g\bar{g}$ states: 6 states made of charged gluons,

$$X\bar{X} \quad (Q = (-1, 0)),$$
$$Y\bar{Y} \quad (Q = (-1/2, -\sqrt{3}/2)),$$
$$Z\bar{Z} \quad (Q = (1/2, -\sqrt{3}/2)),$$
$$\bar{X}X (Q = (1, 0)),$$
$$\bar{Y}Y \quad (Q = (1/2, \sqrt{3}/2)),$$
$$\bar{Z}Z \quad (Q = (-1/2, \sqrt{3}/2)),$$

and 4 states with $Q = (0, 0)$ made of neutral gluons,

$$AA, \quad BB, \quad AB, \quad BA.$$

So for quarks the operator s is 3×3 matrix, and for gluons it is 10×10 matrix.

For a given background field (i. e., before averaging over the color fields) the s-matrix element averaged over the thermal states of the QGP can be written as

$$\Big\langle\Big\langle\langle\{1\}|s(\boldsymbol{\rho},\Delta L,0,\boldsymbol{\rho},f)|\{1\}\rangle\Big\rangle\Big\rangle_{th} = \\ = \sum_{\psi_1,\ldots,\psi_{M+1}} \langle\{1\}|\psi_{M+1}\rangle\times \\ \times\,\Phi(\boldsymbol{\rho},h/2,Q_{M+1},f)\langle\psi_{M+1}|V_M(\boldsymbol{\rho},h)|\psi_M\rangle \\ \times\,\Phi(\boldsymbol{\rho},h,Q_M,f)\ldots\Phi(\boldsymbol{\rho},h,Q_3,f)\langle\psi_3|V_2(\boldsymbol{\rho},h)|\psi_2\rangle\times \\ \times\,\Phi(\boldsymbol{\rho},h,Q_2,f)\langle\psi_2|V_1(\boldsymbol{\rho},h)|\psi_1\rangle\times \\ \times\,\Phi(\boldsymbol{\rho},h/2,Q_1,f)\langle\psi_1|\{1\}\rangle\,, \quad (57)$$

where the operator V_i reads (the index i indicates that the operator acts at the longitudinal coordinate $z=z_i$)

$$V_i(\boldsymbol{\rho},h) = \hat{1} - \frac{nh}{2}\hat{\sigma}(\boldsymbol{\rho})\,. \quad (58)$$

The formula (58) corresponds to the first order term of the standard Glauber series, that appears after averaging over positions of the scattering centers. One can introduce the total phase factor $\Phi_{tot}(\boldsymbol{\rho},h,\{Q\},f)$ defined as the product of the phase factors Φ for all the intermediate states ψ_i, for the set of the color charges $\{Q\}=(Q_{M+1},\ldots,Q_1)$ corresponding to the color charges of the parton p in the set of the intermediate states $\{\psi\}=(\psi_{M+1},\ldots,\psi_1)$. Then, the matrix element of the operator s averaged over the thermal states and over the color Lorentz force f can be written as

$$\Big\langle\Big\langle\langle\{1\}|s(\boldsymbol{\rho},\Delta L,0,f)|\{1\}\rangle\Big\rangle\Big\rangle = \\ = \sum_{\psi_1,\ldots,\psi_{M+1}} \langle\{1\}|\psi_{M+1}\rangle\langle\psi_{M+1}|V_M(\boldsymbol{\rho},h)|\psi_M\rangle\cdots\times \\ \times\,\langle\psi_3|V_2(\boldsymbol{\rho},h)|\psi_2\rangle\langle\psi_2|V_1(\boldsymbol{\rho},h)|\psi_1\rangle\langle\psi_1|\{1\}\rangle\times \\ \times\,\Big\langle\Big\langle\Phi_{tot}(\boldsymbol{\rho},h,\{Q\},f)\Big\rangle\Big\rangle_f, \quad (59)$$

where the averaged of the color Lorentz force factor Φ_{tot} (calculated using the Gaussian distribution (55)) reads

$$\Big\langle\Big\langle\Phi_{tot}(\boldsymbol{\rho},h,\{Q\},f)\Big\rangle\Big\rangle_f = \\ = \exp\Big\{-\frac{\boldsymbol{\rho}^2g^2\sigma^2h^2}{4}\sum_{a=3,8}\Big[\sum_{k=1}^{M+1}\eta_kQ_k^a\Big]^2\Big\} \quad (60)$$

with $\eta_k=1/2$ for $k=1$ and $M+1$, and $\eta_k=1$ for $1<k<M+1$.

The $\langle\mathbf{p}^2\rangle$ for one slab of the QGP with the background field in terms of s reads

$$\langle\mathbf{p}^2\rangle = -4\frac{d}{d\rho^2}\times \\ \times\ln\Big[\Big\langle\Big\langle\langle\{1\}|s(\boldsymbol{\rho},\Delta L,0,f)|\{1\}\rangle\Big\rangle\Big\rangle\Big]\Big|_{\rho\sim1/q_{max}}. \quad (61)$$

To calculate $\langle\mathbf{p}^2\rangle$ uing (61) we write the operator V as

$$V(\boldsymbol{\rho},h) = V(0,h) + v(\boldsymbol{\rho},h) \quad (62)$$

with $v(\boldsymbol{\rho},h)=V(\boldsymbol{\rho},h)-V(0,h)$. Using (41) and (58) we obtain at small $\boldsymbol{\rho}$

$$V_{\alpha\bar{\alpha}}^{\beta\bar{\beta}}(0,h) = \delta_\alpha^\beta\delta_{\bar{\alpha}}^{\bar{\beta}} - \\ - \frac{nhC_RC_tg^4}{32\pi m_D^2}\Big[\delta_\alpha^\beta\delta_{\bar{\alpha}}^{\bar{\beta}} - \frac{(T_R^a)_\alpha^\beta(T_{\bar{R}}^a)_{\bar{\alpha}}^{\bar{\beta}}}{C_R}\Big], \quad (63)$$

$$v_{\alpha\bar{\alpha}}^{\beta\bar{\beta}}(\boldsymbol{\rho},h) \approx -\frac{\rho^2hn_q^{eff}C_2(\rho_{min})}{2C_R}(T_R^a)_\alpha^\beta(T_{\bar{R}}^a)_{\bar{\alpha}}^{\bar{\beta}} = \\ = -\frac{\rho^2h\hat{q}_R}{4C_R}(T_R^a)_\alpha^\beta(T_{\bar{R}}^a)_{\bar{\alpha}}^{\bar{\beta}}\,. \quad (64)$$

In (64) we used that $\hat{q}=2nC_2$. Note that $V(\boldsymbol{\rho}=0,h)\neq\hat{1}$ because the operator $\hat{\sigma}(\boldsymbol{\rho})$ given by (41) does not vanish at $\boldsymbol{\rho}=0$ (only its expectation value between color singlet states vanishes at $\boldsymbol{\rho}=0$). Note that the $V(0,h)$ can be rewritten in terms of the parton mean free path in the QGP $\lambda_{mfp}=1/n\sigma_p$ as

$$V_{\alpha\bar{\alpha}}^{\beta\bar{\beta}}(0,h) = \delta_\alpha^\beta\delta_{\bar{\alpha}}^{\bar{\beta}} - \\ - \frac{h}{\lambda_{mfp}}\Big[\delta_\alpha^\beta\delta_{\bar{\alpha}}^{\bar{\beta}} - \frac{(T_R^a)_\alpha^\beta(T_{\bar{R}}^a)_{\bar{\alpha}}^{\bar{\beta}}}{C_R}\Big], \quad (65)$$

with

$$\lambda_{mfp}^{-1} = n\int_0^{q_{max}^2}dq^2\frac{d\sigma_p}{dq^2} \approx \frac{nC_RC_tg^4}{32\pi m_D^2}\,. \quad (66)$$

The λ_{mfp} characterizes the length of the color randomization of the parton p in the QGP [49]. Note that λ_{mfp} defined by (66) is smaller that the mean free path λ in the formula of the kinetic theory [28, 29] for η (1). The latter is related to the transport cross section

$$\lambda^{-1} = n\sigma_p^{tr}$$

with

$$\sigma_p^{tr} = \int d\sigma_p sin^2\theta \approx \frac{4}{s}\int d\sigma_p q^2,$$

which is smaller than the total cross section entering (66). Note that the HTL counterpart of (66), defined by

$$\lambda^{-1}_{mfp}\Big|_{HTL} \approx \frac{g^2 C_R T}{4\pi}\int\limits_0^{q^2_{max}} dq^2 C(q^2) \qquad (67)$$

gives logarithmically divergent λ^{-1}_{mfp} for the standard HTL formula for $C(q^2)$ derived in [48]

$$C(q^2) = \frac{1}{q^2} - \frac{1}{q^2+m_D^2}\,. \qquad (68)$$

This occurs due to the $1/q^2$ term in (68), which comes from the transverse part of the gluon polarization tensor Π_T, and is related to the absence of screening for the transverse static gluons, i.e., due to zero magnetic screening mass, defined in the HTL scheme as

$$m_M^2 = \mathrm{Re}\Pi_T(0) = 0,$$

see [48]. In general, it is invalid [50]. In [48] it was suggested to account for the nonzero magnetic mass in the HTL calculation of the factor C by using $\mathrm{Re}\Pi_T(0) = m_M^2$ with nonzero m_M. This leads to

$$C(q^2) = \frac{1}{q^2+m_M^2} - \frac{1}{q^2+m_D^2}\,. \qquad (69)$$

Substituting this into (67), we obtain

$$\lambda^{-1}_{mfp}\Big|_{HTL,m_M\neq 0} \approx \frac{g^2 C_R T}{4\pi}\ln\Big(\frac{m_D^2}{m_M^2}\Big)\,. \qquad (70)$$

Lattice calculations of [51, 52] give $m_D/m_M \sim 2-3$. This can lead to a sizeable logarithmic increase of λ_{mfp} for the HTL scheme with magnetic mass as compared to the model with the static color centers [45]. Note that the sensitivity of the color relaxation time (and conductivity) to the ratio m_D/m_M was discussed long ago in [49].

From (61) using (59), (60), (63) and (64) we obtain for one slab

$$\langle \mathbf{p}^2\rangle = \langle \mathbf{p}^2\rangle_{th} + \langle \mathbf{p}^2\rangle_f\,, \qquad (71)$$

where $\langle \mathbf{p}^2\rangle_{th,f}$ correspond to p_T broadening due to rescatterings on the thermal QGP constituents and scattering in the background turbulent field affected by the color randomization due to particle rescatterings on the thermal partons. The thermal contribution, which comes from v, reads

$$\langle \mathbf{p}^2\rangle_{th} = -\frac{Mh\hat{q}_R}{C_R}\{1\}^{\bar\beta}_{\beta}(T^a_R)^{\beta}_{\alpha}(T^a_{\bar R})^{\bar\beta}_{\bar\alpha}\{1\}^{\bar\alpha}_{\alpha} = \Delta L\hat{q_R}\,. \qquad (72)$$

To obtain (72), we used that in (59), without the phase factor Φ_{tot}, all the intermediate projectors $|\psi_k\rangle\langle\psi_k|$ can be replaced by $|\{1\}\rangle\langle\{1\}|$. In this case, the right hand side of (59) in the limit of small ρ becomes

$$\langle\{1\}|V(0,h)+v(\boldsymbol{\rho},h)|\{1\}\rangle^M \approx \approx 1 + M\langle\{1\}|v(\boldsymbol{\rho},h)|\{1\}\rangle\,, \qquad (73)$$

that, after substitution into (61), leads to (72) (which agrees with calculations of the thermal p_T given in section 2, as it must be). The $\langle \mathbf{p}^2\rangle_f$ term in (71) comes from the Taylor expansion of the phase factor Φ_{tot} and the matrix elements of $V(0,h)$ in (59). Using (59), (60) and (61) one can obtain

$$\langle \mathbf{p}^2\rangle_f = h^2g^2\sigma^2\times \times \sum_{\psi_1,\ldots,\psi_{M+1}} \langle\{1\}|\psi_{M+1}\rangle\langle\psi_{M+1}|V(0,h)|\psi_M\rangle\cdots\times \times \langle\psi_3|V(0,h)|\psi_2\rangle\langle\psi_2|V(0,h)|\psi_1\rangle\langle\psi_1|\{1\}\rangle\times \times \sum_{a=3,8}\Big[\sum_{k=1}^{M+1}\eta_k Q_k^a\Big]^2. \qquad (74)$$

The background field contribution to the transport coefficient is

$$\hat{q}_R^f = \frac{\langle p_T^2\rangle_f}{\Delta L}.$$

The formula (74), together with (63), can be used for numerical calculation of the turbulent contribution to the transport coefficient. Note that for quarks summing over the color index a in the second term inside the square brackets in (63) can be performed analytically with the help of the Fierz identity for triplet color generators:

$$(\mathbf{t}^a)^l_m(\mathbf{t}^a)^i_k = \frac{1}{2}\delta^i_m\delta^l_k - \frac{1}{2N_c}\delta^i_k\delta^l_m.$$

For gluon color generators we performed summing over a in (63) numerically.

In the absence of rescatterings we have $V(0,h)=1$ (see Eq. (63), and (74) is reduced to

$$\langle \mathbf{p}^2\rangle_f = h^2M^2g^2\sigma^2\sum_{a=3,8}\langle Q^{a2}\rangle_{\{1\}}\,. \qquad (75)$$

From this relation, using

$$\langle\{1\}|Q_3^2+Q_8^2|\{1\}\rangle = \frac{2C_R}{N_c^2-1},$$

we obtain in our model without the thermal contribution

$$\hat{q}_R = \frac{2C_R\Delta L g^2\sigma^2}{N_c^2-1}\,. \qquad (76)$$

This prediction agrees with formula (29) because in our model

$$\left\langle\left\langle \tilde{F}^a_{i+}(z)\tilde{F}^a_{i+}(0)\right\rangle\right\rangle = \left\langle\left\langle \tilde{F}^a_{i+}(0)\tilde{F}^a_{i+}(0)\right\rangle\right\rangle \cdot F(z) \quad (77)$$

with

$$\left\langle\left\langle \tilde{F}^a_{i+}(0)\tilde{F}^a_{i+}(0)\right\rangle\right\rangle = 2\sigma^2\,,$$

and

$$F(z) = \begin{cases} 1-|z|/\Delta L & \text{if } |z|<\Delta L\,, \\ 0 & \text{if } |z|>\Delta L\,. \end{cases} \quad (78)$$

It is worth noting that the formulas (77) and (78) show that our simplified model of the random background fields nevertheless leads to a quite reasonable form of the field strength correlation function. For this reason, one can expect that the use of the multilayer homogeneous fields cannot greatly distort the results.

Note, finally, that although in our model we use a specific geometry for the color exchanges, physically, it is evident that it cannot be crucial for our predictions. Because the only important quantity for the magnitude of the effect of the color randomization on p_T broadening is the ratio $\Delta L/\lambda_{mfp}$, which is clearly insensitive to the specific choice of the z-distribution of the color exchanges of the fast parton in a slab.

4. NUMERICAL RESULTS

In this section, we present numerical results for $\hat{q}$ using formulas of previous section[2)]. We use the QCD coupling constant $g = 2$. To characterize the magnitude of the background color field we use the ratio of the chromomagnetic field energy density $\epsilon_f = B^2/2$ to the total QGP energy density $\alpha = \epsilon_f/\epsilon_{tot}$. We define the total QGP energy density in terms of the equilibrium temperature in the ideal gas model:

$$\epsilon_{tot} = (\frac{8\pi^2}{15} + \frac{7\pi^2 N_f}{20})T^4 \approx 13.9T^4$$

(we take $N_f = 2.5$). We assume that the magnetic field is isotropic. In this case for the Gaussian parameter σ in (55) we have $\sigma^2 = (2/3)\alpha\epsilon_{tot}$. We perform calculations of $\hat{q}$ for $T = 350$ MeV, which seems to be reasonable for the initial stage of the QGP evolution at $\tau \sim 1-2$ fm for heavy ion collisions at the LHC energies. In the absence of realistic calculations of the turbulent QCD matter evolution in AA collisions, the characteristics of the turbulent magnetic fields can not be obtained theoretically. We perform calculations for for $\alpha = 0.2$ and 0.3. Such values of α can lead to reasonable values of the ratio η/s in the scenario with the dominant contribution of the turbulent fields to the QGP shear viscosity [21–23]. The ratio of the chromomagnetic energy to the total QGP energy substantially higher than $0.2-0.3$ looks unrealistic.

For quarks we perform calculations of $\hat{q}$ for ΔL in the interval between 0.5 to 2 fm. We present the results obtained for the number of slices (in Eq. (57)) $M = 15$. For the HTL version with $m_D/m_M = 3$, that has the smallest λ_{mfp}, the estimated errors are $\lesssim 2\%$ at $L \sim 2$ fm, and are $\lesssim 0.5\%$ at $L \lesssim 1$ fm (for $m_D/m_M = 2$ the errors becomes smaller by a factor of $\sim 2-3$). For the static model even at $L \sim 2$ fm the errors are $\lesssim 0.3\%$. For gluons the needed computational resources are considerably larger than for quarks (for the same value of M). For this reason we performed calculations for $M = 10$. For the HTL version we restricted the maximal values of ΔL ($\Delta L < 1.1(1.5)$ fm for $m_D/m_M = 3(2)$) to avoid regions where the errors may be too large. For the static model we present the results for the interval $0.5 < \Delta L < 2$ fm (in this interval the estimated errors are $\lesssim 3\%$ at $L \sim 2$ fm, and are $\lesssim 0.7\%$ at $L \lesssim 1$ fm).

In Figs. 4–7 we present results for the contribution to $\hat{q}$ for quark and gluon from scattering on the thermal constituents, and from scattering in the random chromomagnetic fields without and with the effect of the parton color randomization. The calculations are performed for the parton energy $E = 50$ GeV. Note that in our model only the thermal contribution to $\hat{q}$ depends on the parton energy (due to the energy dependence of the Coulomb logarithm). From Figs. 4–7 one can see that the effect of the parton color randomization reduces the turbulent contribution to $\hat{q}$ by a factor of ~ 0.8 at $\Delta L \sim 1$ and ~ 0.65 at $\Delta L \sim 2$ fm for the static model (the reduction is approximately the same for quarks and gluons). For the HTL scheme the effect is stronger. For $m_D/m_M = 2(3)$, the color randomization reduces the turbulent $\hat{q}$ for quarks by a factor of 0.7(0.6) at $\Delta L \sim 1$ fm and by a factor of 0.5(0.4) at $\Delta L \sim 2$ fm. The magnitude of the reduction of the turbulent $\hat{q}$ for gluons due to the color randomization at $\Delta L \sim 1$ fm in the HTL scheme is similar to that for quarks.

Note that, since the turbulent contribution to $\hat{q}$ is approximately energy independent, one can expect that our results should be valid for the thermal partons as well. The effect of the parton color randomization should lead to some increase of the turbulent

[2)] Note that our numerical calculations demonstrated that for gluons the last two states made of color neutral gluons AB and BA do not contribute to $\hat{q}$, i.e., for gluons calculations can be performed with 8×8 matrix.

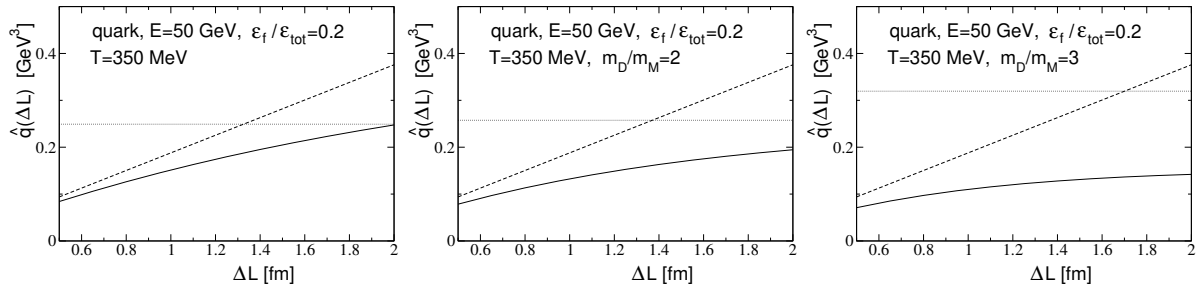

Fig. 4. The transport coefficient $\hat{q}$ for quark with energy $E = 50$ GeV in the QGP with $T = 350$ MeV, $\epsilon_f/\epsilon_{tot} = 0.2$ as a function of ΔL for the static model (left) and for the HTL scheme with $m_D/m_M = 2$ (middle) and $m_D/m_M = 3$ (right). Solid line: the turbulent contribution to $\hat{q}$ obtained accounting for the color randomization of the fast parton; dashed line: the turbulent contribution without the color randomization of the fast parton; dashed line: the thermal contribution

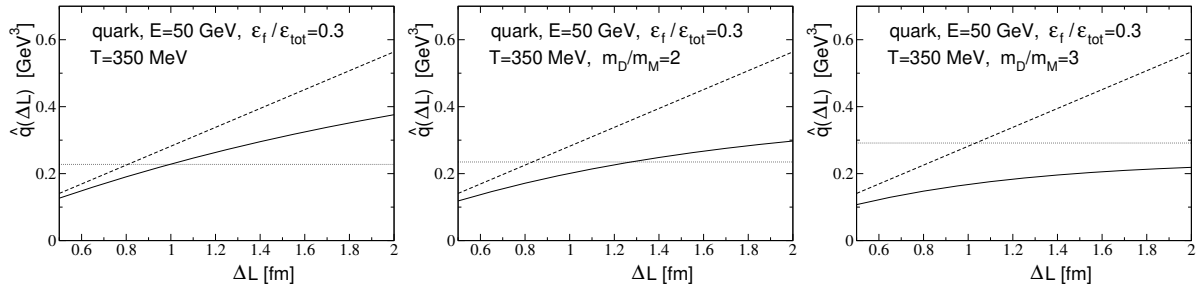

Fig. 5. The same as in Fig. 4 for $\epsilon_f/\epsilon_{tot} = 0.3$

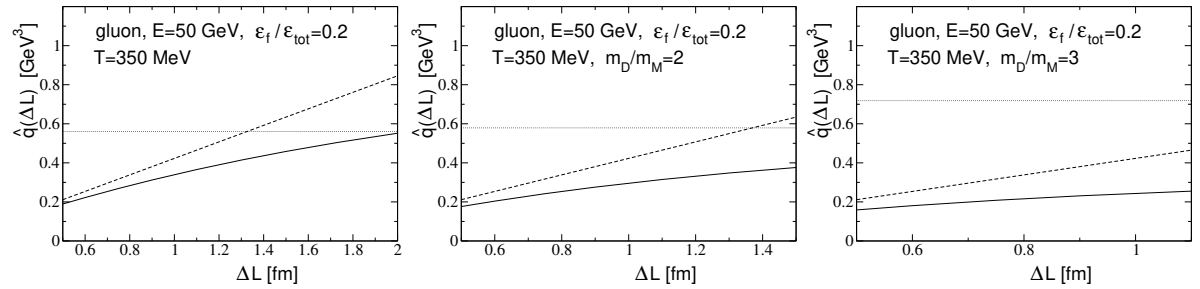

Fig. 6. The same as in Fig. 4 for gluon

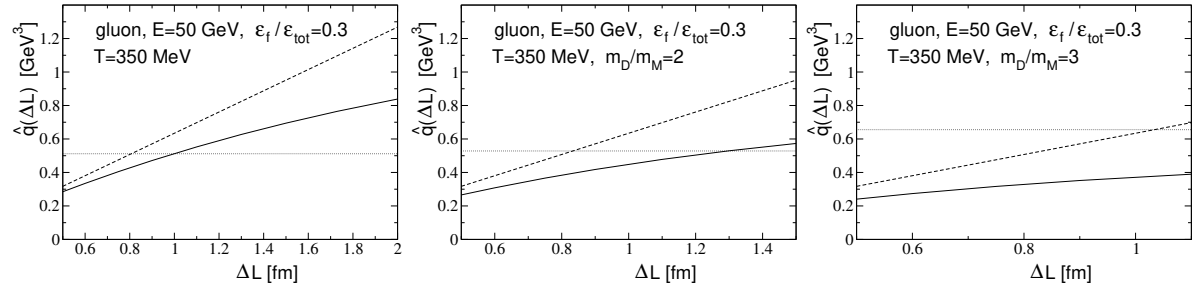

Fig. 7. The same as in Fig. 5 for gluon

shear viscosity as compared to predictions without the color randomization (like that of [21,22]). For the HTL scheme with $m_D/m_M = 2(3)$ the ratio η/s should become bigger by a factor of $\sim 1.2 - 1.5(1.3 - 1.8)$ for $\Delta L \sim 0.5 - 1$ fm.

Finally, it is worth noting that the suppression of $\hat{q}_f$ due to the color randomization of fast partons may be enhanced by the effects of the running coupling, that have been ignored in the present analysis. The lattice calculations of [53] show that at small virtualities the in-medium α_s may grow up to $\sim 0.5 - 0.8$. The growth of α_s at low momenta (and the perturbative logarithmic decrease at high momenta) is more important for the parton color randomization length λ_{mfp} entering (65) than for the thermal transport coefficient $\hat{q}_{th}$ (for which the relative contribution of the low momentum region is suppressed by the factor q^2). For this reason, the suppression effect of the color randomization on the turbulent contribution to $\hat{q}$ should be bigger for the scheme with the running coupling (if the models with the fixed and the running coupling lead to similar predictions for the thermal transport coefficient).

5. CONCLUSIONS

We have analyzed the effect of the parton color randomization on the p_T broadening of fast partons in the QGP with turbulent color fields that can be generated in the QGP formed in AA collisions due to the non-abelian Weibel instabilities. Calculations of the transverse momentum broadening of a fast parton traversing the turbulent QGP ignoring its interaction with the QGP constituents give the transport coefficient $\hat{q}$ approximately proportional to the product of the mean field energy ϵ_f and the correlation length r_c of the turbulent color fields. The gluon exchanges between the fast parton and the thermal partons change the color charge of the fast parton, that lead to random variation of the Lorentz force experienced by the fast parton. This acts as a reduction of the correlation length of the turbulent color fields, and reduces the transport coefficient.

We performed calculations of $\hat{q}$ for a simplified model of fluctuating color fields in the form of alternating sequential transverse layers of thickness ΔL of homogeneous transverse chromomagnetic fields with random orientation in the SU(3) group, and gaussian distribution in the magnitude. We demonstrated that calculation of $\hat{q}$ may be reduced to calculation of p_T broadening in a single layer. We presented the one-layer $\langle p_T^2 \rangle$ in a form which is convenient for numerical simulations. We performed calculations using for the color exchanges between the fast parton and the thermal partons the static model of the Debye screened color centers [45] and the HTL scheme [47] with a nonzero magnetic mass [48]. Our numerical results show that the color randomization can lead to a sizable reduction of the turbulent contribution to $\hat{q}$. We find that the reduction of $\hat{q}$ due to the color randomization is bigger for the HTL scheme, for which the effect grows with increasing m_D/m_M. For the HTL version with $m_D/m_M = 3$ we obtained the suppression of the turbulent contribution to $\hat{q}$ by a factor of ~ 0.6 for $\Delta L \sim 1$ and ~ 0.4 for ~ 2 fm. We have found that the reduction of the turbulent contribution to $\hat{q}$ due to the parton color randomization is very similar for quarks and gluons. The magnitude of the suppression is weakly dependent on the average energy of the turbulent color fields in the QGP.

Funding. This work is supported by the State program FFWR-2024-0011.

REFERENCES

1. R. Derradi de Souza, T. Koide, and T. Kodama, Prog. Part. Nucl. Phys. **86**, 35 (2016) [arXiv:1506.03863].

2. P. Romatschke and U. Romatschke, *Relativistic Fluid Dynamics In and Out of Equilibrium*, Cambridge Monographs on Mathematical Physics, Cambridge University Press, (2019), ISBN: 978-1-108-48368-1, 978-1-108-75002-8, DOI: 10.1017/9781108651998 [arXiv:1712.05815].

3. U. Heinz and R. Snellings, Ann. Rev. Nucl. Part. Sci. **63**, 123 (2013) DOI: 10.1146/annurev-nucl-102212-170540 [arXiv:1301.2826].

4. P. Kovtun, D.T. Son, and A. O. Starinets, Phys. Rev. Lett. **94**, 111601 (2005) [hep-th/0405231].

5. H. Song, S. A. Bass, U. Heinz, and T. Hirano, Phys. Rev. C **83**, 054910 (2011) , Erratum: Phys. Rev. C **86**, 059903 (2012) DOI: 10.1103/PhysRevC.86.059903, 10.1103/PhysRevC.83.054910 [arXiv:1101.4638].

6. P. B. Arnold, G. D. Moore, and L. G. Yaffe, JHEP **11**, 001 (2000) [hep-ph/0010177].

7. D. Molnar and M. Gyulassy, Nucl. Phys. A**697**, 495 (2002), Nucl. Phys. A**703**, 893 (2002) (erratum) [nucl-th/0104073].

8. P. B. Arnold, G. D. Moore, and L. G. Yaffe, JHEP **05**, 051 (2003) [hep-ph/0302165].

9. J. Ghiglieri, G. D. Moore, and D. Teaney, JHEP **03**, 179 (2018) [arXiv:1802.09535].

10. S. Caron-Huot, Phys. Rev. D **79**, 065039 (2009) [arXiv:0811.1603].

11. Z. Xu and C. Greiner, Phys. Rev. Lett. **100**, 172301 (2008) [arXiv:0710.5719].

12. Z. Xu and C. Greiner, Phys. Rev. C **71**, 064901 (2005) [hep-ph/0406278].

13. R. Baier, A.H. Mueller, D. Schiff, and D.T. Son, Phys. Lett. B **502**, 51 (2001) [hep-ph/0009237].

14. P. B. Arnold, J. Lenaghan, and G. D. Moore, JHEP **08**, 002 (2003) [hep-ph/0307325].

15. S. Mrowczynski, Acta Phys. Polon. B **37**, 427 (2006) [hep-ph/0511052].

16. P. Romatschke and M. Strickland, Phys. Rev. D **68**, 036004 (2003) [hep-ph/0304092].

17. S. Mrówczyński, Phys. Lett. B **214** 587 (1988); *ibid.* B **393**, 26 (1997); Phys. Rev. C **49**, 2191 (1994).

18. E. S. Weibel, Phys. Rev. Lett. **2**, 83 (1959).

19. P. B. Arnold and G. D. Moore, Phys. Rev. D **76**, 045009 (2007) [arXiv:0706.0490].

20. P. Arnold and G. D. Moore, Phys. Rev. D **73**, 025006 (2006) [hep-ph/0509206].

21. M. Asakawa, S. A. Bass, and B. Muller, Phys. Rev. Lett. **96**, 252301 (2006) [hep-ph/0603092].

22. M. Asakawa, S. A. Bass, and B. Muller, Prog. Theor. Phys. **116**, 725 (2007) [hep-ph/0608270].

23. A. Majumder, B. Muller, and X.-N. Wang, Phys. Rev. Lett. **99**, 192301 (2007) [hep-ph/0703082].

24. B. Muller and D.-L. Yang, Acta Phys. Polon. Supp. **16**, 37 (2023) [arXiv:2207.14504].

25. S. Mrowczynski, B. Schenke, and M. Strickland, Phys. Rept. **682**, 1 (2017) [arXiv:1603.08946].

26. I. Dremin, M. Kirakosyan, and A. Leonidov, Adv. High Energy Phys. **2013**, 706521 (2013) [arXiv:1305.3812].

27. R. Baier, Y. L. Dokshitzer, A. H. Mueller, S. Peigné, and D. Schiff, Nucl. Phys. B **484**, 265 (1997) [hep-ph/9608322].

28. F. Reif, *Fundamentals of Statistical and Thermal Physics,* McGraw-Hill (1965).

29. P. Danielewicz and M. Gyulassy, Phys. Rev. D **31**, 53 (1985).

30. B. Muller, Phys. Rev. D **104**, L071501 (2021) [arXiv:2107.14775].

31. B. G. Zakharov, JETP Lett. **88**, 475 (2008) [arXiv:0809.0599].

32. M. E. Carrington, S. Mrowczynski, and B. Schenke, Phys. Rev. C **95**, 024906 (2017) [arXiv:1607.02359].

33. S. K. Wong, Nuovo Cim. A **65**, 689 (1970).

34. A. Ipp, D. I. Müller, and D. Schuh, Phys. Rev. D **102**, 074001 (2020) [arXiv:2001.10001].

35. B. G. Zakharov, Sov. J. Nucl. Phys. **46**, 92 (1987).

36. B. G. Zakharov, JETP Lett. **63**, 952 (1996) [hep-ph/9607440]; *ibid.* **65**, 615 (1997) [hep-ph/9704255]; *ibid.* **70**, 176 (1999) [hep-ph/9906536]; Phys. Atom. Nucl. **61**, 838 (1998) [hep-ph/9807540].

37. R. P. Feynman and A. R. Hibbs, it Quantum Mechanics and Path Integrals, McGRAW–HILL Book Company, New York (1965).

38. Y. Aharonov and D. Bohm, Phys. Rev. **115**, 485 (1959).

39. H. Liu, K. Rajagopal, and U. A. Wiedemann, Phys. Rev. Lett. **97**, 182301 (2006) [hep-ph/0605178].

40. H. Liu, K. Rajagopal, and U. A. Wiedemann, JHEP **03**, 066 (2007) [hep-ph/0612168].

41. Ya. Aref'eva, Theor.Math. Phys. **43**, 353 (1980).

42. N. E. Bralić, Phys. Rev. D **22**, 3090 (1980).

43. P. M. Fishbane, S. Gasiorowicz, and P. Kaus, Phys. Rev. D **24**, 2324 (1981).

44. Yu. A. Simonov, Sov. J. Nucl. Phys. **50**, 134 (1989) [Yad. Fiz. **50**, 213 (1989)].

45. M. Gyulassy and X. N. Wang, Nucl. Phys. B **420**, 583 (1994) DOI: 10.1016/0550-3213(94)90079-5 [nucl-th/9306003].

46. M. H. Thoma, Rev. Mod. Phys. **81**, 959 (2009) [arXiv:0801.0956].

47. E. Braaten and R. D. Pisarski, Nucl. Phys. B **337**, 569 (1990); B **339**, 310 (1990); J. Frenkel, J. C. Taylor, Nucl. Phys. B **334**, 199 (1990); Nucl. Phys. B **374**, 156 (1992).

48. P. Aurenche, F. Gelis and H. Zaraket, JHEP **0205**, 043 (2002) [hep-ph/0204146].

49. A. V. Selikhov and M. Gyulassy, Phys. Lett. B **316**, 373 (1993) [nucl-th/9307007].

50. D. J. Gross, R. D. Pisarski, and L. G. Yaffe, Rev. Mod. Phys. **53**, 13 (1981).

51. Y. Maezawa et al. [WHOT-QCD Collaboration], Phys. Rev. D **81**, 091501 (2010) [arXiv:1003.1361].

52. A. Nakamura, T. Saito, and S. Sakai, Phys. Rev. D **69**, 014506 (2004) [hep-lat/0311024].

53. A. Bazavov et al., Phys. Rev. D **98**, 054511 (2018) DOI: 10.1103/PhysRevD.98.054511 [arXiv:1804.10600].